J|A|C|S
COMMUNICATIONS

Published on Web 05/19/2006

Solution Properties of Graphite and Graphene

Sandip Niyogi, Elena Bekyarova, Mikhail E. Itkis, Jared L. McWilliams, Mark A. Hamon, and Robert C. Haddon*

Department of Chemistry, Department of Chemical and Environmental Engineering, and Center for Nanoscale Science and Engineering, University of California, Riverside, California 92521-0403

Received January 29, 2006; E-mail: robert.haddon@ucr.edu

Recent transport measurements indicate that graphene has great promise as an electronic material.[1−3] Graphene is the hypothetical infinite aromatic sheet of sp^2-bonded carbon that is the 2-D counterpart of naturally occurring 3-D graphite.[4] It is found in the π-stacked hexagonal structure of graphite with an interlayer spacing of 3.34 Å, which is the van der Waals distance for sp^2-bonded carbon. The interlayer cohesive energy or exfoliation energy for pyrolytic graphite has been experimentally determined as 61 meV/C atom.[5] The area occupied by a carbon atom in graphite is $(3^{3/2}/4)$-l^2,[6] where l is the carbon−carbon bond length (0.1421 nm);[7] thus, a 1-nm square of graphene contains about 38 carbon atoms, and the separation energy of two 1-nm squares of graphene is over 2 eV. Graphene itself does not occur naturally and prior work on the fabrication of electronic devices has primarily relied on the physical separation of the sheets or on preparation under specialized conditions.[1−3,8−10] In the present communication we show that chemistry offers opportunities for overcoming these very large cohesive energies and provides attractive routes for the manipulation of functionalized graphene.

Commercially available microcrystalline graphite exists as extremely hydrophobic 1−20 μm particles that aggregate into thin films on contact with solvent.[11] When treated under strongly oxidizing acidic conditions, graphite oxide is formed.[12,13] Structurally, graphite oxide is an epoxidized form of the sp^2-bonded carbon network together with acidic functional groups at the edges with the oxidants intercalated in the interlaminar space; this leads to a route for the exfoliation of graphite by rapid de-intercalation.[13,14] Variations of this oxidative route have been studied in the quest to find applications for graphite oxide.[11,15−18] The materials formed unstable dispersions and the thickness of the graphitic films had a minimum value of 1.4 nm.[15−18]

As a part of our interest in the dissolution of carbon materials, we have explored the derivatization of graphite, following the procedure we previously demonstrated for the chemical processing of single-walled carbon nanotubes.[19,20] We find that exfoliation with strong acid, followed by functionalization with a long-chain alkylamine gives rise to stable solutions of this material in organic solvents.

Microcrystalline graphite (Aldrich, 5 g) was sonicated in 120 mL of a 3:1 mixture of H_2SO_4 (18 M) and HNO_3 (17 M) for 2 h, in a Cole-Parmer cup-horn sonicator at a power level of 200 W, while maintaining the temperature at 40 °C. The dispersion was allowed to stand at room temperature for 4 days during which time the color of the dispersion turned purple−brown. After repeated washing with water (total 4 L), by centrifugation and decantation, the oxidized graphite was filtered through a 0.2 μm PTFE membrane, with a final ethanol wash. The product was allowed to dry under vacuum overnight; the material had a grayish appearance and was not as shiny as the starting material.

Oxidized graphite from the acid reaction (100 mg), was refluxed in 20 mL of $SOCl_2$ in the presence of 0.5 mL of *N*,*N*-dimethylformamide (DMF), at 70 °C for 24 h, using a $CaCl_2$ guard tube. At the end of the reaction, the excess $SOCl_2$ was removed by distillation, and 67 mg of the product was allowed to react with 545 mg of octadecylamine (ODA) at 120 °C for 4 days. The product was dispersed in hot ethanol, filtered through a 0.2 μm PTFE membrane, and washed with 200 mL of hot ethanol. The dried product was dissolved in 50 mL of THF and filtered through a Fisher P8 coarse filter paper. The yield of the reaction was 20 wt %, with respect to the oxidized graphite. The product octadecylamido graphite, G-CONH$(CH_2)_{17}CH_3$ has a solubility of 0.5 mg/mL in THF and is also soluble in CCl_4 and 1,2-dichloroethane.

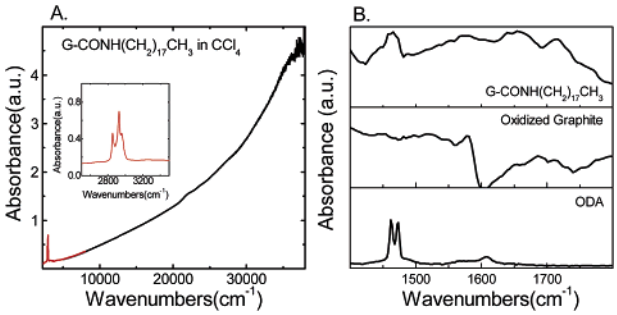

Figure 1. (A) Absorption spectrum of a CCl_4 solution of G-CONH$(CH_2)_{17}$-CH_3 at a concentration of 0.156 mg/mL, measured in a quartz cell of 1 cm path length. The spectrum from 2500 to 6000 cm^{-1} was collected on a Nicolet Nexus FT-IR spectrometer and from 5000 to 38000 cm^{-1} on a Varian Cary500 spectrophotometer, using the same sample. (Inset) Absorbance associated with the asymmetric C−H stretch of the alkyl groups. (B) Mid-IR spectra collected from thin films on ZnSe of product and the starting materials.

The absorption spectrum of the G-CONH$(CH_2)_{17}CH_3$ in carbon tetrachloride is shown in Figure 1A. The electronic absorption processes associated with the π-valence and conduction bands in graphite, show a maximum around 4.2 eV, similar to previous solid-state observations[21] and to the calculated optical absorption spectrum.[22] We observe the asymmetric C−H stretch of the alkyl groups at 2854 and 2925 cm^{-1}; the corresponding bands in free ODA occur at 2848 and 2918 cm^{-1}. The mid-IR spectra of films of G-CONH$(CH_2)_{17}CH_3$, the acid-oxidized graphite, and free ODA are shown in Figure 1B. The peak at 1653 cm^{-1} in the G-CONH-$(CH_2)_{17}CH_3$ corresponds to carbonyl stretch of the amide, although the signals corresponding to the acidic form in the oxidized graphite are weak.

The graphite solutions obey Beer's law (Figure 2), and for the G-CONH$(CH_2)_{17}CH_3$ the extinction coefficient (ϵ) was determined to be 40 L mol^{-1} cm^{-1} at 10 000 cm^{-1}. Dispersions of the oxidized graphite were not very stable, but a value of $\epsilon = 46$ L mol^{-1} cm^{-1} (10 000 cm^{-1}) was found. Earlier spectroscopic studies of thin sections of graphitic coal gave similar low values for the extinction coefficient;[23,24] for single-walled carbon nanotubes, values of $\epsilon \approx$ 400 L mol^{-1} cm^{-1} were determined.[25] It is important to note the different spectral character of the dispersions; clearly, the length

10.1021/ja060680r CCC: $33.50

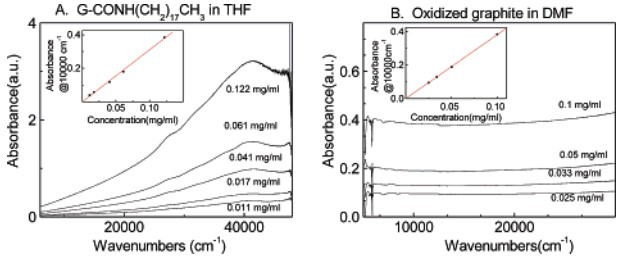

Figure 2. Absorption spectra as a function of concentration. (A) G−CONH$(CH_2)_{17}CH_3$ in THF; (B) dispersions of oxidized graphite in DMF.

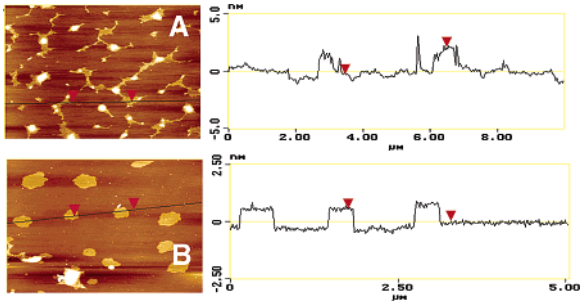

Figure 3. Tapping mode AFM height images of soluble graphite on mica. Two components were observed, (A) 1.5−2.5 nm thick G_n films and (B) G_1 sheets of (uncorrected) height 5.3 Å.

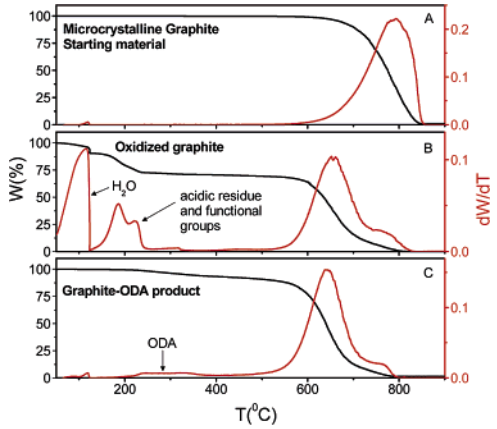

Figure 4. Thermogravimetric analysis data, under dry air with a temperature ramp rate of 10 °C/min. (A) Graphite starting material has an oxidation onset at 700 °C. (B) Acid-oxidized graphite suffers significant weight loss at 600 °C. Residual water is removed at 120 °C, and acidic residues and functional groups are oxidized between 180 and 220 °C. (C) High-temperature bulk oxidation of G-CONH$(CH_2)_{17}CH_3$ is similar to (B), with an additional feature due to the loss of the organic functionalities between 220 and 350 °C.

scale of the oxidized graphite particles is sufficient to scatter the incident light, thereby producing the featureless spectrum seen in Figure 2B.

To characterize the soluble species, THF solutions were evaporated on mica and examined by AFM (Figure 3); the solutions consisted of irregular graphite crystallites (G_n) with a measured thickness of 1.5−2.5 nm (Figure 3A) and circular graphene layers (G_1) with a measured height of ∼5.3 Å (Figure 3B). The acid oxidation reaction is known to etch graphitic crystallites into the larger structures observed in the present study.[11,15,16] We note that previous AFM observations of G_1 found a thickness of 3.4 Å[26] and 4 Å with a dead space of 5 Å, between graphene and the substrate that is occupied by trapped solvent.[1] The extensive edge functionalization employed in our approach may be expected to increase the dead space and thus, we expect that the material imaged in Figure 3B is composed of single-layer graphene sheets.

The thermogravimetric analysis shows that the starting graphite oxidizes at ∼800 °C (Figure 4A); after acid oxidation reaction, the bulk material oxidizes at ∼600 °C, with substantial weight loss around 200 °C due to the loss of the acidic functional groups and residues (Figure 4B).[18] The G-CONH$(CH_2)_{17}CH_3$ product shows a 7 wt % loss around 300 °C (Figure 4C), due to the oxidative decomposition of the organic functional groups.

Acknowledgment. This work was supported by DOD/DARPA/DMEA under award number DMEA90-02-2-0216.

References

(1) Novoselov, K. S.; Geim, A. K.; Morozov, S. V.; Jiang, D.; Zhang, Y.; Dubonos, S. V.; Grigorieva, I. V.; Firsov, A. A. *Science* **2004**, *306*, 666−669.
(2) Berger, C.; Song, Z.; Li, T.; Li, X.; Ogbazghi, A. Y.; Feng, R.; Dai, Z.; Marchenkov, A. N.; Conrad, E. H.; First, P. N.; de Heer, W. A. *J. Phys. Chem. B* **2004**, *108*, 19912−19916.
(3) Zhang, Y.; Tan, Y. W.; Stormer, H. L.; Kim, P. *Nature* **2005**, *438*, 201−204.
(4) Debye, P.; Scherrer, P. *Phys. Z.* **1917**, *18*, 291−301.
(5) Zacharia, R.; Ulbricht, H.; Hertel, T. *Phys. Rev. B* **2004**, *69*, 155406.
(6) Haddon, R. C.; Brus, L. E.; Raghavachari, K. *Chem. Phys. Lett.* **1986**, *131*, 165−169.
(7) Dresselhaus, M. S.; Dresselhaus, G.; Eklund, P. C. *Science of Fullerenes and Carbon Nanotubes*; Academic Press: San Diego, 1996.
(8) Dujardin, E.; Thio, T.; Lezec, H.; Ebbesen, T. W. *App. Phys. Lett.* **2001**, *79*, 2474−2476.
(9) Zhang, Y.; Small, J. P.; Amori, M. E. S.; Kim, P. *Phys. Rev. Lett.* **2005**, *94*, 176803.
(10) Zhang, Y.; Small, J. P.; Pontius, W. V.; Kim, P. *Appl. Phys. Lett.* **2005**, *86*, 073104.
(11) Kotov, N. A.; Dekany, I.; Fendler, J. H. *Adv. Mater.* **1996**, *8*, 637−641.
(12) Brodie, B. C. *Philos. Trans. R. Soc. London* **1859**, *149*, 249−259.
(13) Mckay, S. F. *J. Appl. Phys.* **1964**, *35*, 1992−1993.
(14) Beckett, R. J.; Croft, R. C. *J. Phys. Chem.* **1952**, *56*, 929−935.
(15) Cassagneau, T.; Fendler, J. H. *Adv. Mater.* **1998**, *10*, 877−881.
(16) Kovtyukhova, N. I.; Ollivier, P. J.; Martin, B. R.; Mallouk, T. E.; Chizhik, S. A.; Buzaneva, E. V.; Gorchinskiy, A. D. *Chem. Mater.* **1999**, *11*, 771−778.
(17) Bourlinos, A. B.; Gournis, D.; Petridis, D.; Szabo, T.; Szeri, A.; Dekany, I. *Langmuir* **2003**, *19*, 6050−6055.
(18) Viculis, L. M.; Mack, J. J.; Mayer, O. M.; Hahn, T.; Kaner, R. B. *J. Mater. Chem.* **2005**, *15*, 974−978.
(19) Chen, J.; Hamon, M. A.; Hu, H.; Chen, Y.; Rao, A. M.; Eklund, P. C.; Haddon, R. C. *Science* **1998**, *282*, 95−98.
(20) Niyogi, S.; Hamon, M. A.; Hu, H.; Zhao, B.; Bhowmik, P.; Sen, R.; Itkis, M. E.; Haddon, R. C. *Acc. Chem. Res.* **2002**, *35*, 1105−1113.
(21) Taft, E. A.; Philipp, H. R. *Phys. Rev.* **1965**, *138*, A197−A202.
(22) Marinopoulos, A. G.; Reining, L.; Rubio, A.; Olevano, V. *Phys. Rev. B* **2004**, *69*, 245419.
(23) Ergun, S.; McCartney, J. T.; Walline, R. E. *Nature* **1960**, *187*, 1014−1015.
(24) McCartney, J. T.; Ergun, S. *J. Opt. Soc. Am.* **1962**, *52*, 197−200.
(25) Zhao, B.; Itkis, M. E.; Niyogi, S.; Hu, H.; Zhang, J.; Haddon, R. C. *J. Phys. Chem. B* **2004**, *108*, 8136−8141.
(26) Hiuara, H.; Ebbesen, T. W.; Fujita, K.; Tanigaki, K.; Takada, T. *Nature* **1994**, *367*, 148−151.

JA060680R